

BIOFIDELITY EVALUATION OF RECENT SIDE IMPACT DUMMIES

Narayan Yoganandan, Frank A. Pintar, Thomas A. Gennarelli

Department of Neurosurgery
Medical College of Wisconsin
and VA Medical Center
Milwaukee, WI, USA

Matthew R. Maltese, Rolf H. Eppinger

National Highway Traffic Safety Administration
US Department of Transportation
Washington, DC, USA

ABSTRACT

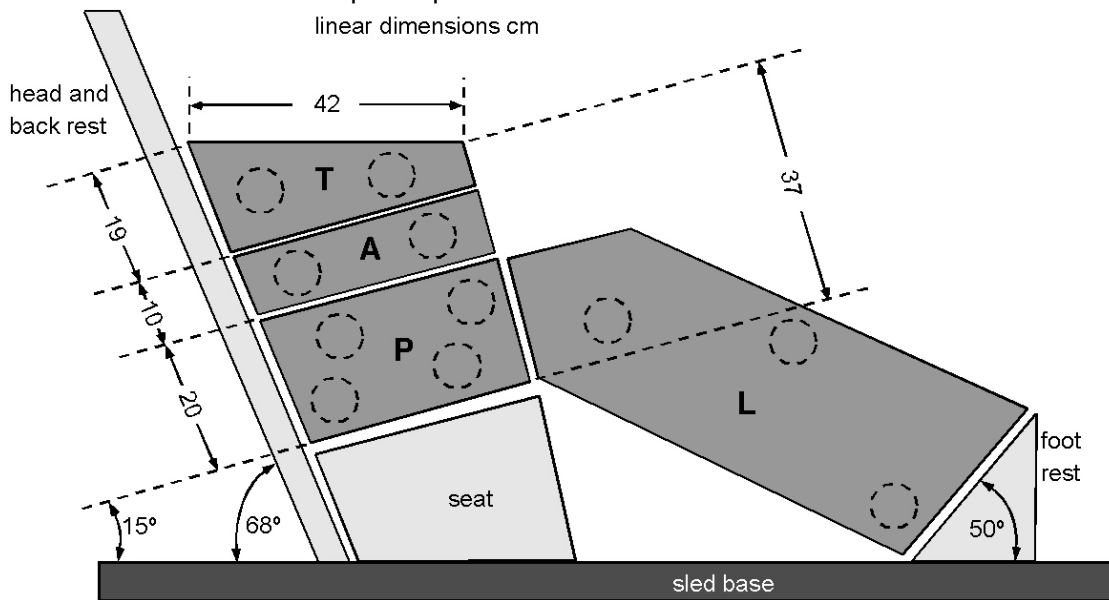
Responses of side impact dummies (SID, BioSID, ES-2, and WorldSIDp) were compared with responses from post mortem human subjects using sled impact tests at a velocity of 6.7 m/s. Test conditions were with and without pelvic offset in combination with and without padding on the impacting wall. Impact forces, thoracic trauma index, chest compression, and viscous criteria were evaluated. The probability of injury was estimated from dummy responses. Rates of deformation were computed for each body region. Dummy responses were not always similar in terms of trend and injury criteria when compared with PMHS tests under the same initial conditions. Response variations will be of value in improving dummy biofidelity.

Key Words: Biomechanics, biofidelity, side impact, injury criteria, dummies

ONE OF THE OBJECTIVES OF SLED TESTING in impact biomechanics is to compare the responses of different surrogates under predetermined initial and boundary conditions in a laboratory environment. Tests are routinely conducted during dummy design to match their responses with responses from post mortem human subjects (PMHS). The dummy is considered biofidelic if its response matches the human subject. This procedure has been in practice for more than three decades of dummy development, regulation, and vehicular component design and evaluation. It is well known that side impact dummies are undergoing constant improvements to enhance their biofidelity characteristics. In fact, an array of dummies exists for side impact assessment including the United States Federalized side impact dummy (SID), second version of the European side impact dummy (ES-2), BioSID impact dummy (BioSID), and WorldSID prototype dummy (WorldSIDp). This research was designed to determine dynamic responses of the side impact dummies currently in use or under development, and compare their responses with PMHS responses in a sled environment to delineate dummy biofidelity.

METHODS

Tests were conducted using a deceleration sled configured with an impacting load wall to simulate side crashes. Dummies were seated on a 1.3-meter long Teflon-coated bench seat rigidly fixed to the platform of the deceleration sled. Figure 1 shows the schematic of the sled buck and load wall. The load wall was configured such that it was flat or had a 110-mm pelvic offset. The test matrix included rigid and padded impacts. All tests were conducted at an impact speed of 6.7 m/s. Details of the sled and methods used in



testing are given in our earlier publications (Pintar et al., 1996; Pintar et al., 1997).

Figure 1: Schematic of the side impact buck with the thoracic (T), abdominal (A), pelvis (P), and extremity (L) plates to measure impact forces from the dummies.

Instrumentation included an accelerometer on the sled to measure change in velocity. Dummy instrumentation included linear displacement transducers in the chest of the ES-2, multiple string potentiometers in the chest of the BioSID, and IR-TRACC infrared

displacement transducers in the chest of the WorldSIDp. Three chestbands were placed on the chest of the SID to obtain deflection data as a function of time during impact. The top two bands were outside the ribs but under the arm foam and jacket. The bottom band was outside the jacket. This process was used to derive chest deformations/contours from which thoracic deflection, velocity, and viscous criteria were computed. Forty to 56 channels of data were collected from each of the three chestbands. Other instrumentation included accelerometers on the sacrum, on the fourth and eighth ribs, and spine. Signals from linear and string potentiometers were filtered using CFC class 600. Accelerometer signals and forces were filtered at SAE class 1000 and 600. Thoracic Trauma Index was computed (Eppinger et al., 1984).

The start of the impact event was defined as the time at which the specific region of the dummy contacted the load wall. For the flat wall tests the thorax load plate was used to determine the start of the impact event and for offset tests the pelvis load plate was used. "Time zero" was defined as follows. The first point on the load-time curve where the force exceeded 200N was determined. Then, starting at the 200N crossing point and progressing backwards in time, the time at which the force reached zero was determined. This process established time-zero for each signal for a particular test.

Chest deflections on the impact side for SID tests were computed as follows. Chest deformation contours were obtained at 250 one-millisecond intervals. On each contour, three locations were selected. Starting at the spine (defined as 0% of contour circumference) and following the contour path in the clockwise direction, locations were marked at 20, 25, and 30% of the circumference. A line was drawn between the sternum (at 50% contour circumference) and spine on each contour, and the three locations identified above were projected onto the sternum-spine line. The distance between each point on the contour on the left side of the thorax and the projected sternum-spine line was measured. The resulting three distances (at 20, 25 and 30% of the circumference) were averaged to find the mean deflection. This process was repeated at all time intervals to generate a left-half chest deflection-time history for each chestband signal. Normalized chest deflections were obtained by dividing the above determined dimensional chest deflection by the one-half depth of the chest of the specific dummy and subsequently filtering the signal using CFC class 600.

For ES-2, BioSID, and WorldSIDp tests, data from internal dummy sensors were used to extract compression histories. The velocity of chest compression was computed by differentiating the SAE class 600-filtered dimensional chest compression signal. The viscous response was obtained by multiplying the velocity signal with the filtered normalized chest compression signal. These procedures are similar to methods described (Yoganandan et al., 1996; Pintar et al., 1997). Peak values of compression, velocity, and viscous criteria obtained using this protocol, were compared with PMHS data.

The effective mass and rate of deformation were compared for each dummy in each test. From the force-time histories of the thorax, abdomen, and pelvis, impulses were computed by integrating the force-time curve. The final time point for the integration was identified as the time at which the force became zero after reaching its peak. The rate of deformation of the specific body region (e.g., thorax) was obtained by integrating the acceleration of the specific body region up to this final time point. Upper spine, lower spine, and pelvic accelerometer data were used for this computation. Dividing the impulse by the rate of deformation for each body region resulted in the effective mass for the region.

In addition, the probability of injury was computed (Kuppa et al., 2000). Assuming the age of the dummy to be 45 years, the logit model (given in the above publication) used

the linear combination of age, normalized chest deflection and resultant spine acceleration for estimating the probability of injury. According to the suggested procedure by Kuppa et al, resultant spine accelerations were filtered at SAE class 180 for the computation of injury probability.

RESULTS

PLOTS of VARIABLES

Responses chosen for the evaluation of the dummies were the peak impact forces and their times of occurrence in the thoracic, abdominal, pelvic and lower extremity regions; acceleration of the upper and lower spine, struck side upper and lower ribs, and pelvis; and deflections from the middle chestband. Corridors from PMHS tests (shown in thicker lines for forces in figures 2a-2d, spinal accelerations in figures 3a and 3b, pelvic accelerations in figure 4, upper and lower rib accelerations in figures 5a and b, and chest deflections in figure 6) were obtained by conducting parallel tests using PMHS. Procedures used to derive the corridors are given (Maltese et al., 2002).

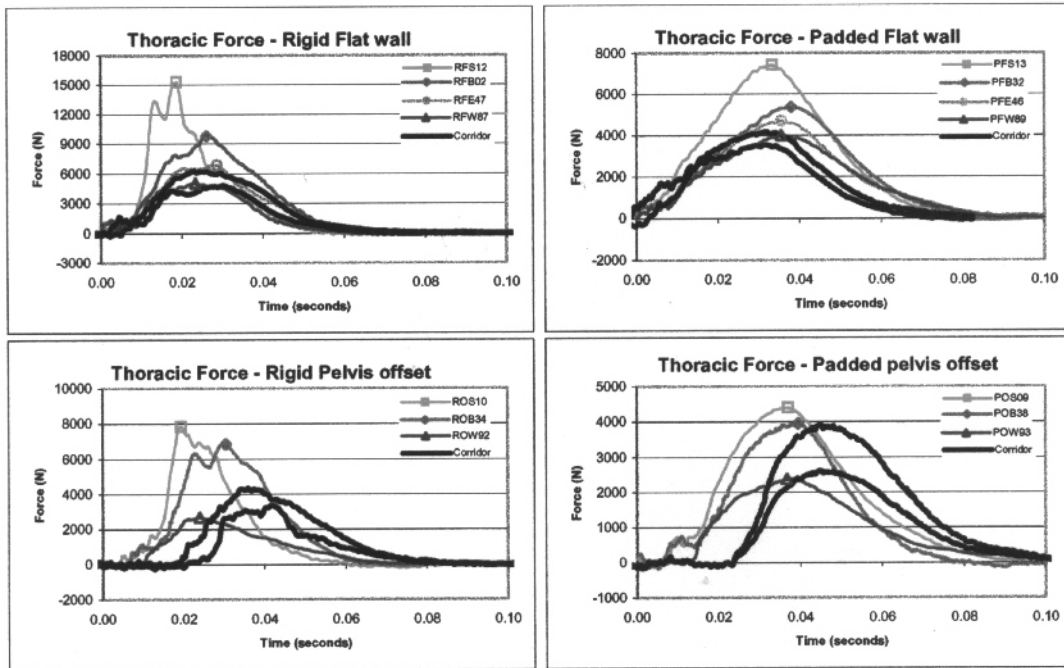


Figure 2a: Thorax forces in rigid flat (RF), padded flat (PF), rigid offset (RO) and padded offset (PO) tests. Dummies are: S: SID, B: BioSID, E: ES-2, and W: WORLDSIDp. Thicker lines in each plot show PMHS corridors.

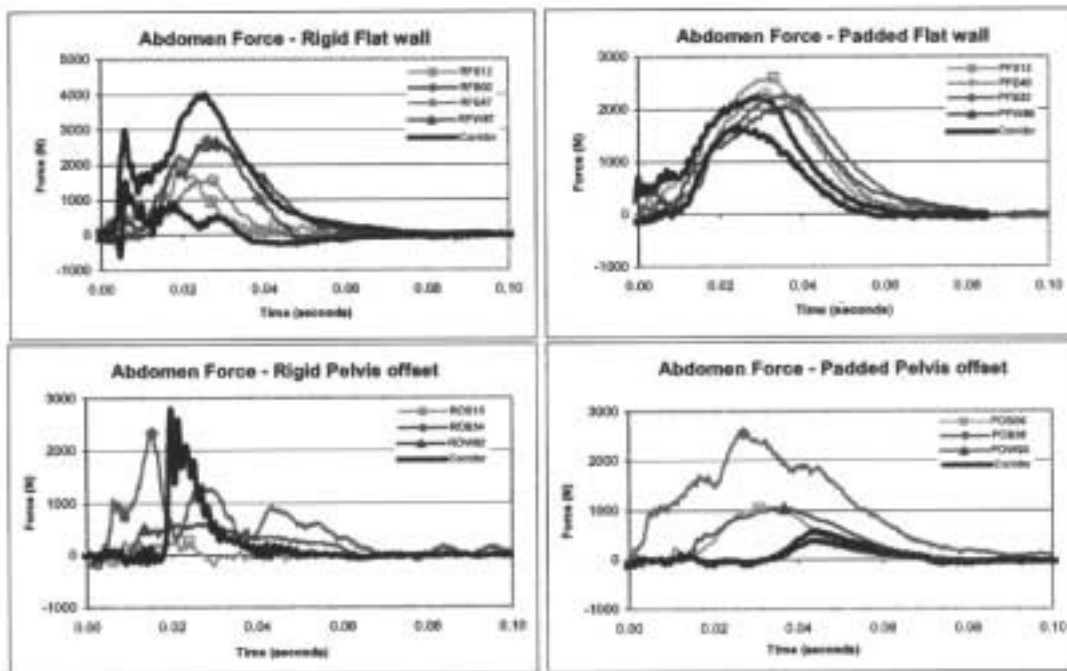


Figure 2b: Abdomen forces in rigid flat (RF), padded flat (PF), rigid offset (RO) and padded offset (PO) tests. Dummies are: S: SID, B: BioSID, E: ES-2, and W: WORLDSIDp. Thicker lines in each plot show PMHS corridors.

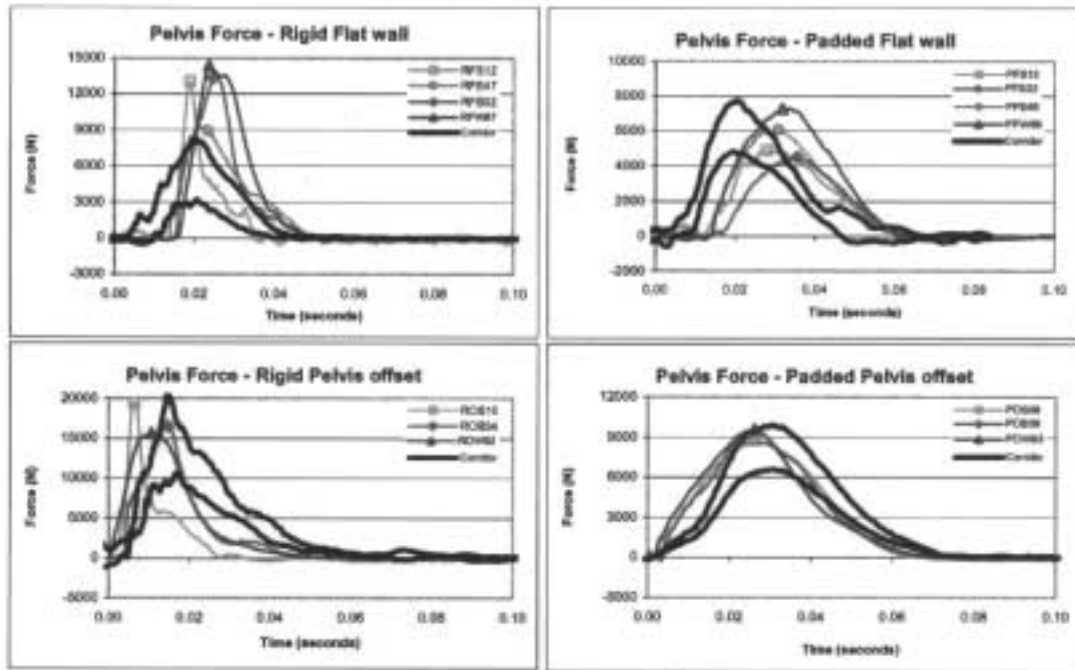


Figure 2c: Forces in the pelvis in rigid flat (RF), padded flat (PF), rigid offset (RO) and padded offset (PO) tests. Dummies are: S: SID, B: BioSID, E: ES-2, and W: WORLDSIDp. Thicker lines in each plot show PMHS corridors.

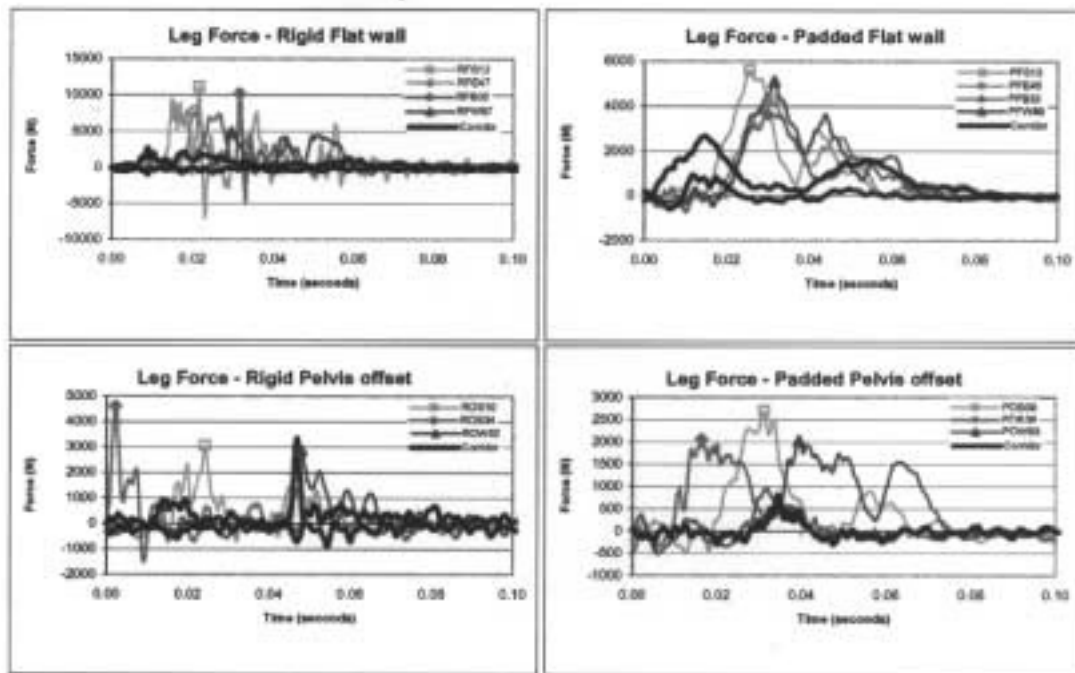


Figure 2d: Extremity forces in rigid flat (RF), padded flat (PF), rigid offset (RO) and padded offset (PO) tests. Dummies are: S: SID, B: BioSID, E: ES-2, and W: WORLDSIDp. Thicker lines in each plot show PMHS corridors.

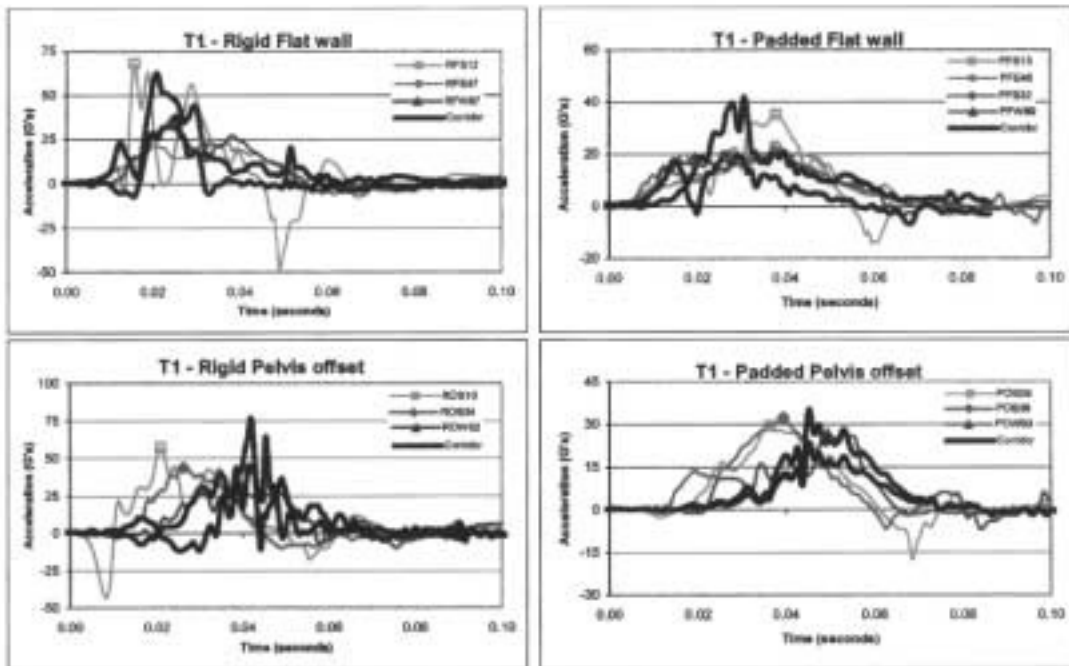


Figure 3a: Upper spine acceleration in rigid flat (RF), padded flat (PF), rigid offset (RO) and padded offset (PO) tests. Dummies are: S: SID, B: BioSID, E: ES-2, and W: WORLDSIDp. Thicker lines in each plot show PMHS corridors.

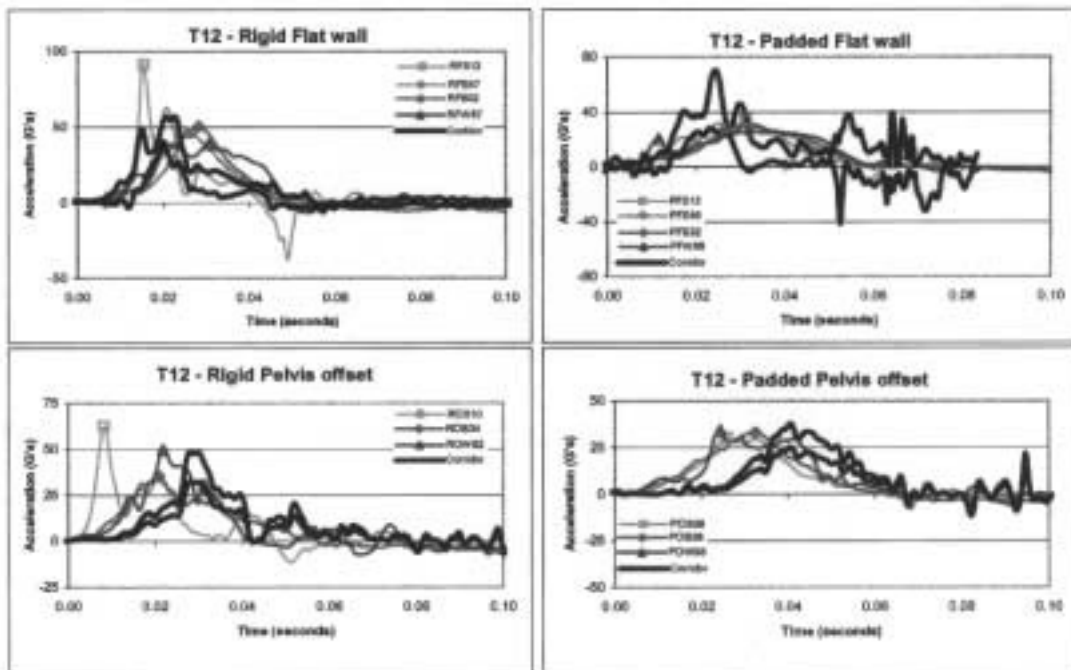


Figure 3b: Lower spine acceleration in rigid flat (RF), padded flat (PF), rigid offset (RO) and padded offset (PO) tests. Dummies are: S: SID, B: BioSID, E: ES-2, and W: WORLDSIDp. Thicker lines in each plot show PMHS corridors.

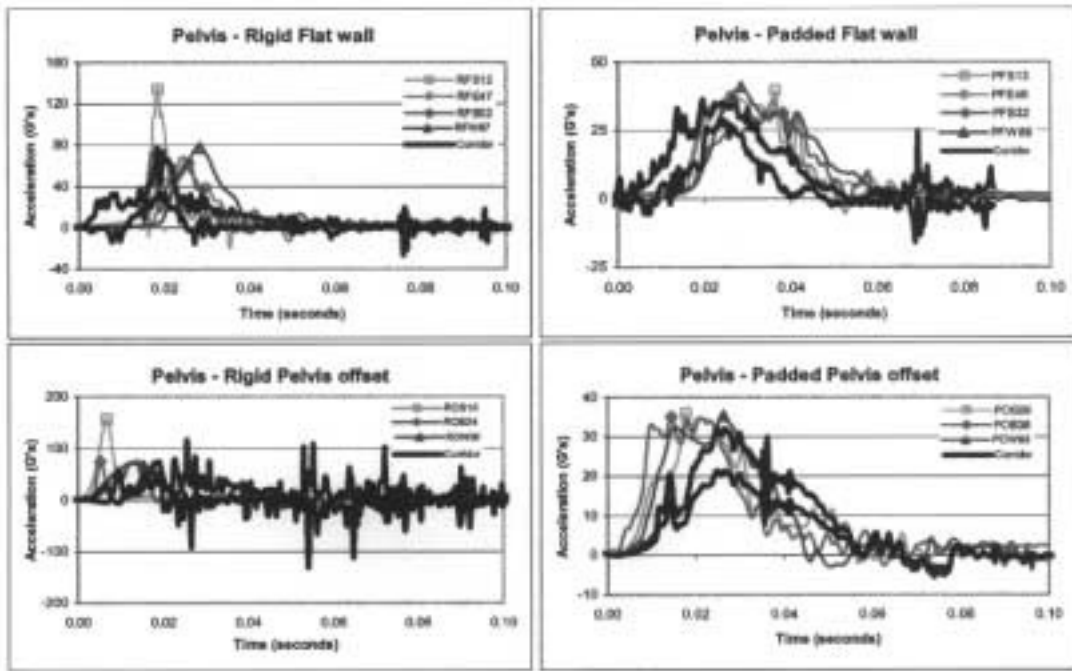


Figure 4: Pelvic acceleration in rigid flat (RF), padded flat (PF), rigid offset (RO) and padded offset (PO) tests. Dummies are: S: SID, B: BioSID, E: ES-2, and W: WORLDSIDp. Thicker lines in each plot show PMHS corridors.

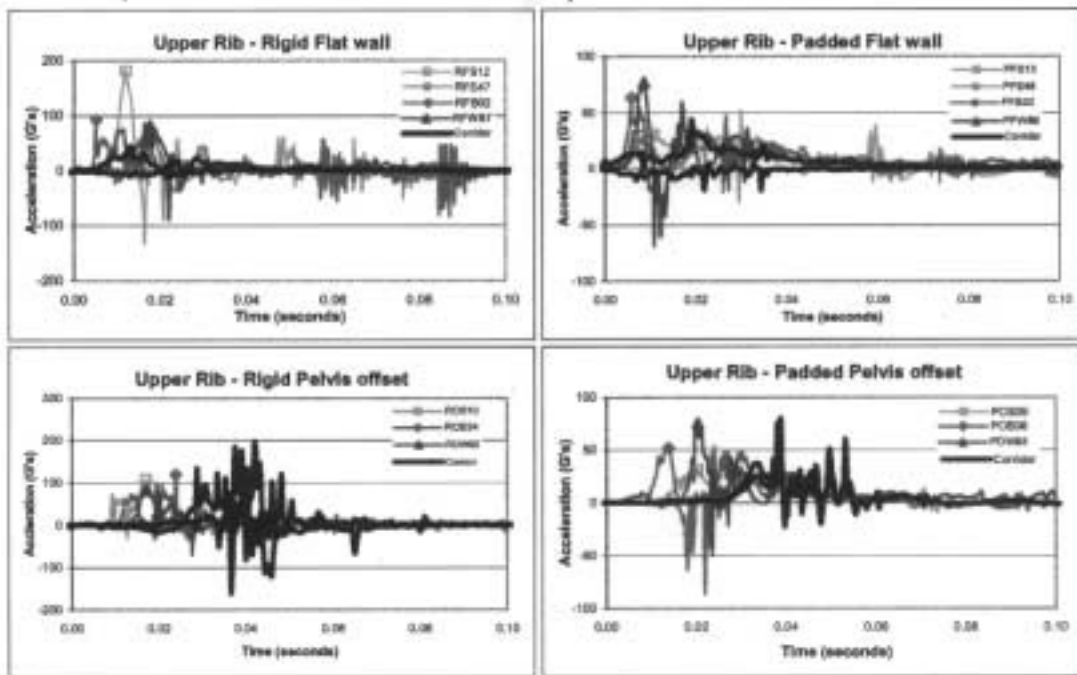


Figure 5a: Upper rib acceleration in rigid flat (RF), padded flat (PF), rigid offset (RO) and padded offset (PO) tests. Dummies are: S: SID, B: BioSID, E: ES-2, and W: WORLDSIDp. Thicker lines in each plot show PMHS corridors.

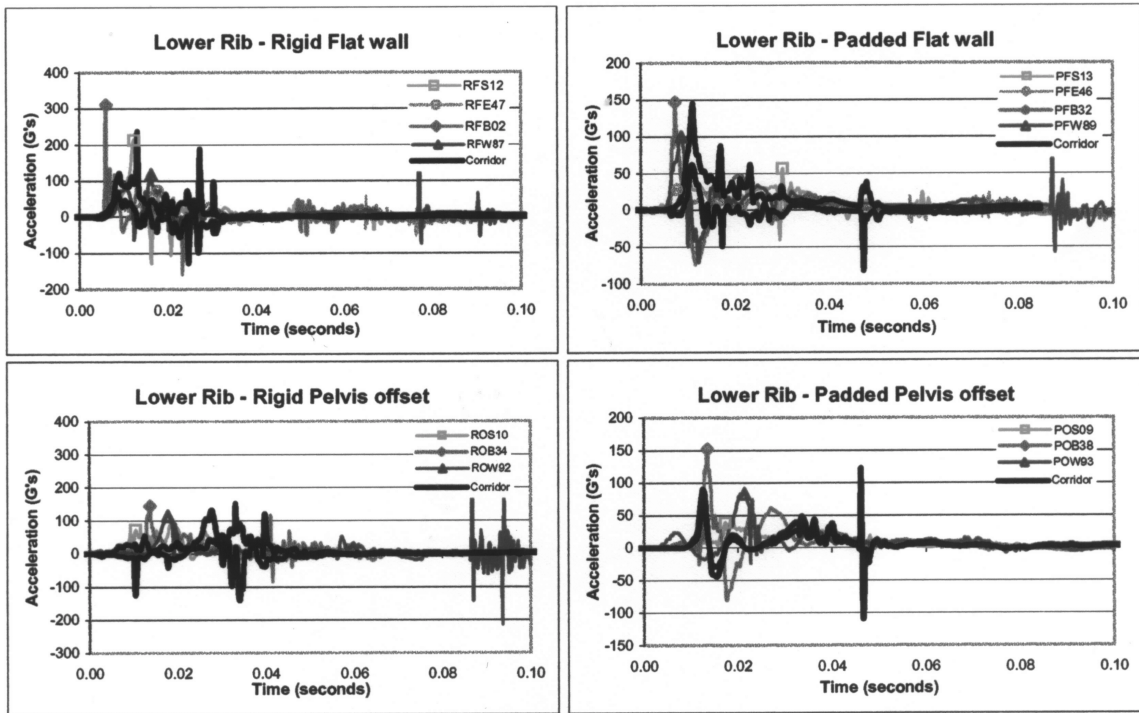


Figure 5b: Lower rib acceleration in rigid flat (RF), padded flat (PF), rigid offset (RO) and padded offset (PO) tests. Dummies are: S: SID, B: BioSID, E: ES-2, and W: WORLDSIDp. Thicker lines in each plot show PMHS corridors.

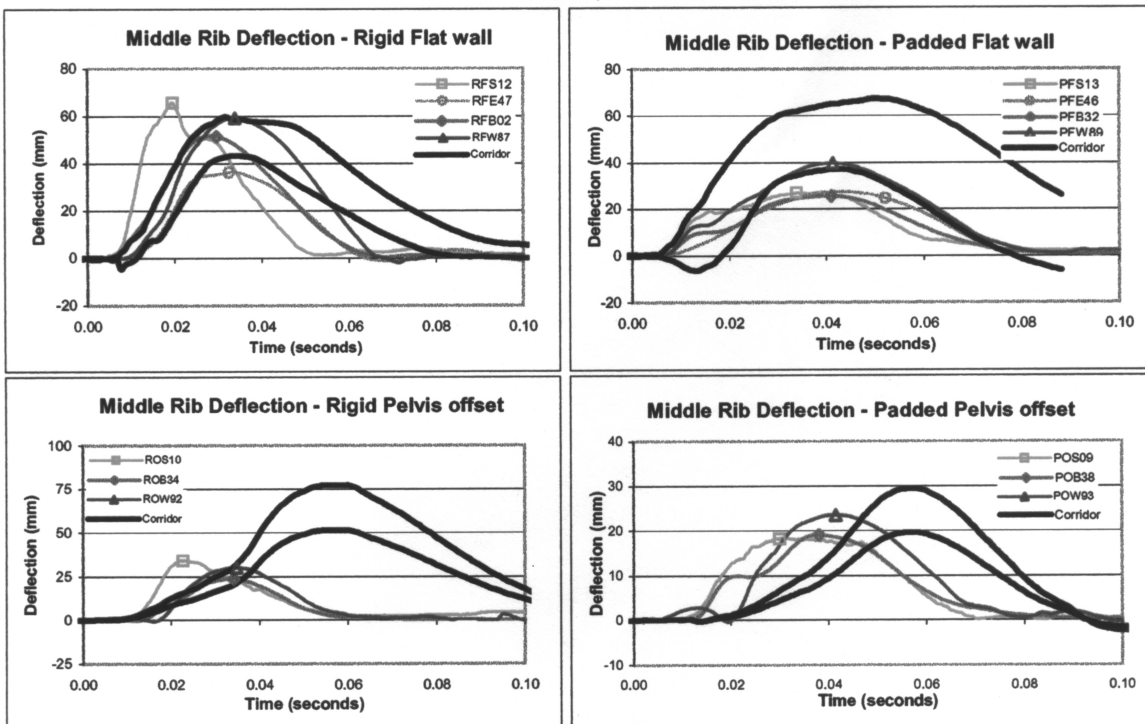


Figure 6: Mid chest deflection in rigid flat (RF), padded flat (PF), rigid offset (RO) and padded offset (PO) tests. Dummies are: S: SID, B: BioSID, E: ES-2, and W: WORLDSIDp. Thicker lines in each plot show PMHS corridors.

Table 1: Data Summary (R: rigid, P: padded, F: flat wall, O: offset, S: SID, B: BioSID, E: ES-2, and W: WorldSIDp).

Test ID	Thorax		Abdomen		Pelvis		Upper left rib		Lower left rib	
	Force (N)	time (ms)	Force (N)	time (ms)	Force (N)	time (ms)	Accl (g)	time (ms)	Accl (g)	time (ms)
RFS12	15282	18.6	2012	20.0	13053	19.0	183.5	11.92	213.4	12.2
RFB02	9819	25.8	2695	25.9	13565	25.0	90.9	4.96	286.5	5.8
RFE47	6891	28.5	1553	27.4	9259	21.1	56.2	12.32	76.7	17.1
RFW87	5092	28.8	2636	28.2	14393	23.4	86.8	16.24	119.0	16.1
ROS10	7845	19.2	283	8.7	19439	6.1	108.3	17.04	92.8	18.6
ROB34	6889	29.8	2321	15.2	16661	14.6	123.1	23.76	147.0	13.5
ROW92	2699	23.6	614	27.4	15708	10.6	85.4	16.80	114.8	17.6
PFS13	7408	33.2	2606	32.9	4872	27.3	52.2	29.84	56.4	29.9
PFB32	5364	37.6	2293	35.4	4546	35.2	59.5	5.68	142.8	7.1
PFE46	4708	35.3	2299	31.0	6057	30.4	28.9	8.08	30.8	7.1
PFW89	3994	35.1	2057	35.8	7276	31.8	76.9	8.56	99.8	8.5
POS09	4399	36.9	1064	32.8	8718	26.2	31.5	20.08	38.9	17.2
POB38	4003	38.2	2592	27.0	8618	28.0	53.2	23.92	151.6	13.4
POW93	2379	36.6	1046	36.3	9593	26.0	79.1	20.16	83.6	21.4
Test ID	Upper spine		Lower spine		Pelvis		Cmax %	VC m/s	TTI g	
	Accl (g)	time (ms)	Accl (g)	time (ms)	Accl (g)	time (ms)				
RFS12	68.0	15.5	92.0	15.2	136.1	18.4	42.2	2.62	104.3	
RFB02	-NA-	-NA-	50.8	27.9	73.7	17.1	35.9	1.08	65.6	
RFE47	23.5	37.0	45.0	26.0	69.2	24.2	27.9	0.71	59.7	
RFW87	33.9	23.8	39.1	21.1	77.7	28.2	40.7	1.42	60.4	
ROS10	57.1	20.9	62.5	8.2	159.2	6.7	33.0	1.04	70.4	
ROB34	43.8	26.1	35.7	20.5	76.3	13.8	14.8	0.27	52.8	
ROW92	30.4	36.3	49.7	21.6	72.6	12.5	29.3	0.80	67.7	
PFS13	35.0	37.7	34.4	31.1	39.6	36.2	19.4	0.46	33.0	
PFB32	20.6	37.8	25.8	33.0	31.9	35.4	19.4	0.30	49.0	
PFE46	23.1	37.6	30.8	30.8	37.4	26.2	22.1	0.19	28.0	
PFW89	20.1	38.6	31.0	32.3	41.0	28.4	26.7	0.45	49.4	
POS09	29.3	36.1	29.9	25.6	35.9	17.6	20.6	1.28	30.8	
POB38	32.5	39.3	33.0	32.6	35.1	14.3	12.5	0.14	53.9	
POW93	26.5	49.0	34.3	24.1	35.4	26.2	20.0	0.33	51.8	
Test ID	Injury Probability (%)		Rate of Deformation (m/s)			Effective Mass (kg)				
	MAIS 3+	MAIS 4+	Thorax	Abdomen	Pelvis	Thorax	Abdomen	Pelvis		
RFS12	23.78	8.18	6.5	7.9	7.5	41.7	3.6	13.5		
RFB02	-NA-	-NA-	-NA-	8.9	7.7	-NA-	6.0	22.9		
RFE47	0.39	0.05	5.9	7.2	7.3	34.8	3.8	21.6		
RFW87	1.44	0.24	7.3	9.8	8.8	23.7	7.6	23.8		
ROS10	1.18	0.19	7.0	6.6	7.3	21.1	0.3	21.8		
ROB34	0.37	0.05	6.6	7.7	6.9	27.4	6.2	36.2		
ROW92	0.42	0.06	7.5	8.2	8.3	10.6	2.4	34.8		
PFS13	0.37	0.05	7.5	8.2	8.8	34.5	9.4	14.8		
PFB32	0.21	0.02	7.4	7.9	7.6	27.8	9.7	15.2		
PFE46	0.28	0.03	7.4	7.7	8.4	25.7	8.9	18.7		
PFW89	0.32	0.04	7.2	9.8	9.4	23.2	7.3	20.7		
POS09	0.24	0.03	6.2	7.3	8.5	25.5	3.7	34.4		
POB38	0.23	0.03	7.2	7.1	8.7	18.3	14.5	33.0		
POW93	0.27	0.03	5.9	8.2	8.5	15.8	4.2	34.8		

INJURY CRITERIA AND PROBABILITY

The probability of MAIS 4+ injury was less than one percent (Table 1) in all cases except the SID for the rigid flat wall test (8.2%). Although the probabilities were very small, the BioSID consistently responded with the lowest probability of injury in all cases. In addition, the SID responded with higher probabilities than the WorldSIDp for flat wall and rigid offset tests and the WorldSIDp responded with higher probabilities than the SID for the padded offset test. A similar trend in data was observed for MAIS 3 category.

TIME SEQUENCE

An evaluation of the time sequence of the attainment of peak forces and accelerations indicated the following. The SID achieved the maximum force earlier than other dummies in rigid wall tests. However, all dummies sustained maximum forces approximately at the same time in padded wall tests. Maximum accelerations in the upper and lower spine and pelvis in the SID occurred before the peak accelerations in the PMHS in all rigid wall (flat and offset) tests (Table 1, Figure 3-4). In contrast, the time of occurrence of peak accelerations in these three regions for the WorldSIDp occurred after the peak PMHS responses in flat wall tests (except pelvis padded condition), and before PMHS in offset tests (except the spines in padded condition).

RATE OF DEFORMATION AND EFFECTIVE MASS

The rate of deformation of the thorax, abdomen and pelvic regions in the WorldSIDp were higher than the SID in all cases (two exceptions, Table 1). For any dummy, the rate of deformation of the pelvis was higher than the rate of deformation of the thorax. The overall rates of deformation for the three regions ranged from 6 to 10 m/s (Table 1). Computation of the effective mass of the thoracic, abdominal, and pelvic regions indicated that the SID produced higher mass than the WorldSIDp for the thorax while the WorldSIDp produced higher mass than the SID for the pelvis in all tests for all conditions. Responses from the other two dummies generally were in between the responses from the WorldSIDp and SID tests (Table 1).

DISCUSSION

Deformations were computed by using chestband contours for the PMHS and SID. The use of the chestband has been demonstrated and validated for frontal and side impacts using PMHS and frontal and side impact dummies (Yoganandan et al., 1991; Morgan et al., 1994; Yoganandan et al., 1994; Pintar et al., 1996; Pintar et al., 1997). This methodology provides surface deformations. Because the internal potentiometer in the SID has a 50-mm deflection limit, chestband data were used to obtain thoracic deflections. In contrast, deflections for the BioSID were obtained from multiple string potentiometers, ES-2 from linear displacement transducers, and WorldSIDp from infrared displacement transducers. These sensors provide internal skeletal rib deflections. All chest deflection output presented in this paper should be interpreted with this focus. Some biomechanical metrics are discussed in the interest of brevity.

Limitations include the determination of biofidelity responses at one impact speed. The PMHS responses exclude active musculature, and if these structures are considered important and deemed critical for dummy design, additional work needs to be conducted. In side impacts, the inactivation of muscles may lead to a conservative estimation of the side impact response because the time to attain the peak response (e.g., force, acceleration) is much lower than the time required for muscle activation. Nonetheless, additional studies

may be needed to confirm this hypothesis. The impact velocity of 6.7 m/s was chosen because of the availability of PMHS tests at this speed. To fully evaluate biofidelity, tests at other velocities are needed. Similarly, tests using other initial conditions such as abdominal and thoracic offset conditions may reveal additional important characteristics.

A general evaluation of the dummy responses with PMHS corridors indicated similarities and variations among dummies and between parameters (e.g., force). Force-time responses of all dummies were similar to PMHS responses (Figures 2a-d). The time of attainment of peak forces in all cases were not identical when compared with the time of occurrence from PMHS tests. In addition, the thoracic force-time responses of all dummies in all tests extended above the PMHS corridors with the exception of the rigid flat wall test with the WorldSIDp (Figure 2a). For the case of the abdominal impact forces, no consistent behavior was apparent. For example, responses from the WorldSIDp and SID matched well for padded offset tests while they differed the most for padded flat wall tests. Pelvic forces also showed characteristic differences with the greatest variations between dummies and PMHS occurring in the rigid flat wall condition (Figure 2c). Although forces in the extremities exhibited variations (Figure 2d), dummy positioning may have played a role. However, these forces during the impact phase were smaller than the thoracic, abdominal, or pelvic impact forces.

An evaluation of the peak impact forces (Table 1, Figure 2) indicated that, in general, the SID sustained higher forces than PMHS in the thorax, abdomen, and pelvis under all impacting conditions (except with the abdomen force for the offset condition). All PMHS data were normalized to 50th percentile occupant mass using scaling laws. Forces in the pelvic and thoracic regions were generally higher than abdominal or extremity regions in all surrogates, and padded tests produced lower forces than rigid tests. Thoracic forces in the WorldSIDp demonstrated closer agreement with PMHS than forces from the other dummies. In contrast, the WorldSIDp did not perform as well as other dummies in pelvic forces under all impacting conditions. The SID consistently demonstrated highest thoracic, abdominal, and pelvic forces in all tests. The BioSID produced the highest abdominal force in padded offset tests than all other dummies. In general, response of the ES-2 was in between the responses of the WorldSIDp and SID dummies.

As expected, padded tests responded with lower chest deflections than rigid tests for flat wall and offset conditions. For the WorldSIDp, maximum normalized chest compression values (C_{max}) occurred at the upper chest level for all tests. In contrast, C_{max} occurred at the lower level for all the other dummies in padded flat wall tests. In rigid flat wall tests, C_{max} occurred at the upper level for the ES-2 and at the lower level for the SID and BioSID tests. All dummies responded with C_{max} at the upper level for the rigid offset tests. While the SID responded with C_{max} at the upper level, the BioSID responded with its C_{max} at the lower level in the padded flat wall tests. These results indicate differing chest compression responses between dummies.

The viscous criterion (VC_{max}) reached its peak for the WorldSIDp in all tests at the upper level with the exception of the rigid flat wall test (lower level). The ES-2 responded with VC_{max} at the lower level in both flat wall tests. The SID responded with VC_{max} at the lower level for the offset and rigid flat wall tests and at the middle level for the padded flat wall test. However, the BioSID responded with peak VC_{max} at the lower level for the padded tests; for the rigid flat wall test peak VC_{max} occurred at the middle level; and for the rigid offset test VC_{max} occurred at the upper level. The differences in the locations of the peaks in the VC_{max} and C_{max} are attributable to the contribution from the velocity component in the VC calculation, indicating its role in side impact injury assessment and mitigation. Nonetheless, differences in dummy responses are readily apparent in injury criteria assessments.

Variations were less in the thoracic trauma index for all dummies for the rigid wall conditions (rigid flat wall TTI 60 to 66 g with one exception; rigid offset TTI 53 to 70 g). Padded tests, however, demonstrated larger variations (padded flat 28 to 49 g; padded offset 31 to 54 g). Increased compliance, i.e., padding, decreased TTI in all dummies except for the pelvic offset in the BioSID. These findings demonstrate the inconsistencies in the dummy responses. Similar conclusions can be drawn from other biomechanical parameters (Figures 2-5).

Several factors may have contributed to differences in magnitudes, patterns, and timing of peak variables in dummy responses. Dummy designs are different. The SID, developed by the US DOT NHTSA, has been in use since the 1970s. It represents the anthropometry of an average US male. The head, neck, spine, and legs are adopted from the Hybrid II 50th percentile male dummy. This dummy is used in US FMVSS 214 regulations. The ES was originally developed in 1989 by a consortium of researchers from the UK, France, Germany, and The Netherlands. The first version of the dummy, ES-1, is used in ECE R95 regulations in Europe. This dummy has been modified in 2000 by TNO and FTSS to accomplish harmonization activities toward uniform standards for side impact injury assessment around the world. The initial intent is to replace ES-1 with ES-2 in ECE95 compliance testing and EuroNCAP programs. The BioSID, developed by the SAE, incorporates the head, neck, and legs from the Hybrid III 50th percentile dummy. This dummy has been used by the industry for side airbag development. In contrast, the WorldSIDp has been in development under the auspices of the ISO since the mid-1990s. The task group formed by the ISO is responsible for the design, development, and continuing validation of the prototype WorldSIDp. The intent is to replace existing side impact dummies with this dummy for worldwide testing and regulation.

Although all dummies represent the 50th percentile male, their weights are not identical (SID 76.5 kg, WorldSIDp 76.7 kg, BioSID 76.1 kg, and ES-2 72 kg). Characteristic design differences in these dummies include the chest, shoulder, lumbar spine, and pelvis. While the SID and ES-2 have no ribs in the abdomen, the other two dummies have each two abdominal ribs. Further, the ES-2 has special padding in the abdominal region. The pelvis of the SID uses the same design as the Hybrid II. However, the unique pelvis design of the WorldSIDp accommodates a sit/stand position. ES-2 rib features include a specially designed triple needle bearing system (Beusenberg et al., 2001). The BioSID and WorldSIDp use six ribs to simulate the shoulder, thoracic and abdominal structures. These structural differences affect the response and biofidelity. For example, the presence of abdominal ribs in the WorldSIDp and BioSID contribute to altered load paths due to impact. Similarly, the lumbar spine construction (rubber without a cable in the WorldSIDp) may change the kinematics and kinetics during impact. Consequently, it is important to evaluate the biofidelity responses of side impact dummies using the present protocol that includes comparisons with PMHS.

CONCLUSIONS

Sled side impact responses of four dummies were compared with PMHS responses. Flat and padded walls with and without pelvic offset conditions were used to evaluate the dummies at a velocity of 6.7 m/s. Impact forces on the thorax, abdomen, pelvis, and extremities, lower and upper spinal, rib, and pelvic accelerations, and left side thoracic deflections were compared with PMHS corridors. Various injury criteria (thoracic trauma index, chest compression, viscous criteria) were evaluated. Responses determined in this study will be of value in improving dummy biofidelity.

- a) Differences existed in the attainment and magnitude of peak forces and accelerations among dummies and PMHS.
- b) Although the probability of MAIS 4+ injury was small, the BioSID consistently responded with the lowest probability of injury. Similar behavior occurred for the MAIS 3+ injury.
- c) The SID responded with higher probabilities of injury than the WorldSIDp for flat wall and rigid offset tests, and the WorldSIDp responded with higher probabilities than the SID for padded offset tests.
- d) The rate of deflection of the thorax, abdomen and pelvic regions in the WorldSIDp were higher than the SID in all cases.
- e) Dummy responses were not always similar in terms of trend and injury criteria when compared with PMHS tests under the same initial condition and velocity.

ACKNOWLEDGMENTS

This study was supported in part by DOT NHTSA DTNH22-93-Y-17028 and VA Medical Research. WorldSIDp tests were conducted in cooperation with the WorldSID Task Group, the EEVC, and Transport Canada.

REFERENCES

- Beusenberg, M., Keown, M. and Yoganandan, N. Improved thorax behaviour of the EUROSID and effects on thorax injury assessment on the basis of pendulum impacts. Int'l Tech Conf on the Enhanced Safety of Vehicles, (2001) Amsterdam.
- Eppinger, R. H., Marcus, J. H. and Morgan, R. M. Development of dummy and injury index for NHTSA's thoracic side impact protection research program. Government/Industrial Meeting and Exposition, (1984) Washington, DC, 1-29.
- Kuppa, S., Eppinger, F., Maltese, M., Naik, R., Yoganandan, N., Pintar, F., Saul, R. and McFadden, J. Assessment of thoracic injury criteria for side impact. IRCOBI, (2000) Montpellier, France, 131-146.
- Maltese, M., Eppinger, R., McFadden, J., Saul, R., Pintar, F., Yoganandan, N. and Hines, M. Response corridors of human surrogates in lateral impacts. Stapp Car Crash Conf, (2002).
- Morgan, R. M., Eppinger, R. H., Haffner, M. P., Yoganandan, N., Pintar, F. A. and Sances, A., Jr. Thoracic trauma assessment formulations for restrained drivers in frontal impact. 38th Stapp Car Crash Conf, (1994) Ft. Lauderdale, FL, Society of Automotive Engineers, Inc., 12-34.
- Pintar, F. A., Yoganandan, N., Hines, M. H., Maltese, M. R., McFadden, J., Saul, R., Eppinger, R., Khaewpong, N. and Kleinberger, M. Chestband analysis of human tolerance to side impact. 41st Stapp Car Crash Conf, (1997) Lake Buena Vista, FL, 63-74.
- Pintar, F. A., Yoganandan, N., Sances, A., Jr and Eppinger, R. H. Instrumentation of human surrogates for side impact. 40th Stapp Car Crash Conf, (1996) Albuquerque, NM, Society of Automotive Engineers, Inc., 29-42.
- Yoganandan, N., Morgan, R. M., Eppinger, R. H., Pintar, F. A., Sances, A., Jr and Williams, A. "Mechanism of thoracic injury in a frontal impact." J Biomech Engr **118**: (1996) 595-597.
- Yoganandan, N., Pintar, F. A., Skrade, D., Chmiel, W., Reinartz, J. M. and Sances, A., Jr. "Thoracic biomechanics with air bag restraint." SAE Transactions **102**(6): (1994) 2597-2607.
- Yoganandan, N., Skrade, D., Pintar, F., Reinartz, J. and Sances, A., Jr. Thoracic deformation contours in a frontal impact. 35th Stapp Car Crash Conf, (1991) San Diego, CA, Society of Automotive Engineers, Inc., 47-63.